

FROM PGA TO ANYTHING: FRAGILITY CURVE CONVERSIONS FOR NUCLEAR POWER PLANT APPLICATIONS

N. D. Karaferis¹, A. V. Gerontati² & D. Vamvatsikos²

¹ School of Civil Engineering, National Technical University of Athens, Greece, nkaraferis@mail.ntua.gr

² School of Civil Engineering, National Technical University of Athens, Greece

Abstract: *There has been a lot of discussion on intensity measure optimality for conventional structures, touting the advantages of novel metrics of ground motion intensity to improve upon the efficiency and fidelity of seismic assessment. Yet, somehow this revolution of sorts has not transitioned to nuclear power plant assessments, which cling to the time-honored tradition of the peak ground acceleration (PGA). They do so for the simple reasons of stiffness and mass. That would be stiffness in the assets themselves, typically leading to periods of the order of 0.1 to 0.2sec for both the structures and their nested components, but also in the rigidity of regulations in an understandably ultra-cautious industry. Adding the mass (and cost) of engineering effort required to reassess already established fragilities for hundreds of standardized components, it is no wonder that there is too much inertia to allow moving away from PGA. Would it not be great if someone came along and offered a minimal-error approach for converting existing fragility curves from PGA to any intensity measure of choice? Interestingly, the response characteristics of nuclear power plants may actually favor an equivalent one/two-degree-of-freedom-model based procedure that allows disaggregating existing fragilities back into ground-motion-level constituents and reconstructing them anew with the desired intensity measure parameterization. There is little doubt that safeguarding the integrity of nuclear power plants would still require massive computations rather than rely on shortcuts, yet such an approach can give novel intensity measures a fighting chance to prove that they are worth the trouble for nuclear engineering.*

1. Introduction

Seismic fragility assessment is a key procedure for engineers to properly quantify the probabilities of reaching or exceeding a predefined level of safety given the intensity. The resulting fragility curves generally provide a useful tool for a performance-based assessment of any structure at hand (e.g. Crowley et al. 2017, Stefanidou and Kappos 2017, Bakalis and Vamvatsikos 2018, Silva et al. 2019, Rosti et al. 2021). The nuclear industry of course exploits these probabilistic techniques as well, applying though a mindset of high conservatism that is more than reasonable given the potential consequences of any damages in a nuclear facility, let alone a nuclear accident. In general, the fragilities employed are based on peak ground acceleration (PGA, e.g. see Zentner et al. 2011, EPRI 2018), as a traditional intensity measure (IM) choice that—given the high stiffness, mass, and elasticity of the structures and components examined—seems to work just fine for their investigations. Despite calling perfection the enemy of good, one shouldn't exclude the implementation of more modern IMs when it comes to the nuclear industry (e.g. see Gerontati and Vamvatsikos 2023). After all, many interesting methodologies and criteria have been presented over time on selecting IMs that better capture the response of a structure (or a portfolio of structures) targeting the best levels of efficiency and sufficiency, e.g., Vamvatsikos and Cornell (2005), Luco and Cornell (2007), Bojórquez and Iervolino (2011), Kazantzi and Vamvatsikos (2015), Eads et al. (2015), Kohrangi et al. (2016), Adam et al. (2017), Bakalis et al. (2018), Heresi and Miranda (2021), O'Reilly (2021), Lachanas et al. (2023).

Understandably though, the process of redesigning the whole assessment process employed by the nuclear community would be very cumbersome and could take years, even to transcend the initial suspicion of

something new replacing something tested and reliable. Matters become even worse if one considers the millions that funding such an endeavour would require, and suddenly the advantages of the status quo staying as it is easily outweighs the benefits of a new perspective. There should be strong evidence that changing a key parameter like the IM is something that would indeed improve on fragilities in a meaningful way and could actually make a real difference to the way the assessment process will progress into the future, for the nuclear community to really start considering moving toward this direction. Whether this is the right step for the industry is something that the authors would rather not attempt to answer for the time being. Instead, they would prefer to focus on presenting a useful tool that would help in reaching a definitive conclusion: A simple methodology to convert the current PGA-based fragility libraries into any IM. Our honest hope is that this can give some breathing space to the concept of a new IM, or at least allow for some more targeted investigations on which is the best IM to base a nuclear facility's assessment.

The methodology to be considered is based on the process of Karaferis and Vamvatsikos (2022, 2023) where an equivalent proxy model is employed to “disaggregate” any fragility into its individual IM-EDP (engineering demand parameter) constituents, for all corresponding seismic records. Having these discrete analysis responses, one can directly recalculate the IM-EDP to correspond to any possible new IM that can be computed via the given ground motion records, and essentially redefine the pre-existing fragility on the basis of this new IM. At face value, the methodology seems to be suitable for the high stiffness, mostly elastic structures of a nuclear power plant (NPP), but herein it will be tested further against a non-structural component (namely a water pump), nested in an NPP structure. Redefining component fragilities with a sufficient accuracy could be a real game changer indeed, when considering that the main risk for such facilities does not really involve structural damages, due to the excessive overstrength of the structures, but rather non-structural ones, especially cases involving different components failing simultaneously. In fact, the above-mentioned methodology will be expanded in the context of this investigation to better capture the component-structure interplay, which is factually the most important seismic parameter that affects component safety.

2. Methodology overview

The method used to disaggregate the fragility curves mainly relies on building a simple equivalent model, using some of the original multi-degree-of-freedom (MDOF) structure's properties. The most important parameters should be the structure's fundamental period, its mass and stiffness, and some information about its global force-deformation behaviour, when the model is nonlinear. In previous examples presented by the authors (Karaferis and Vamvatsikos 2022, 2023) the model was selected to be a one mass model (OMM, see Figure 1a), not because it would be the most accurate choice every time, but because of its simplicity. A complex model would defeat the purpose of this, by nature, approximate method; after a certain point of adding complexities to an equivalent model, one could argue that building a properly defined detailed model would be more straightforward. Still, for the special case of fragilities characterizing nested components in a supporting structure, one could argue that a two-mass model (TMM, see Figure 1b) could be a better suited choice, and thus this model will be also put into the test for the purposes of this study.

In any case this equivalent model will then be used as a proxy to run dynamic analyses, using a set of records that may be generic or characteristic of the site, to produce corresponding “global” EDP values that are representative of the original MDOF structure. This may be performed, e.g., via incremental dynamic analysis (IDA, Vamvatsikos and Cornell 2002). Using those responses paired with their corresponding PGA values, and of course a properly selected capacity threshold (EDP_{lim}), one can theoretically replicate the original fragility of the structure. Though normally, due to the model being extensively simplified, the resulting fragility is unlikely to match the MDOF structure's target fragility. Hence, proper calibration of the equivalent model's results would be required. Assuming a lognormal fragility model, the correction parameters proposed to match the target fragility are the following:

- α : a correction factor, meant to adjust (multiply) the adopted EDP_{lim} threshold to ensure that the median IM of the equivalent-model lognormal fragility matches the median of the MDOF target fragility.
- β_α : an additional dispersion, added to the record-to-record variability in a square-root-sum-of-squares fashion to ensure that the total equivalent-model fragility dispersion matches the (normally) higher dispersion of the MDOF target fragility.

These values are calculated via an iterative calibration process, described in detail in Karaferis and Vamvatsikos (2022). After calibrating, the IM-EDP pairs that correspond to the final α -adjusted EDP_{lim} value should by now faithfully represent the original fragility. Then, the assumption is that if one employs the corresponding records to transform each pair into new IM coordinates, these new IM values would still correspond to the same EDP_{lim} and would thus recreate a good representation of the MDOF fragility, regardless of the IM applied. Figure 2 presents a visual representation of how the methodology is structured.

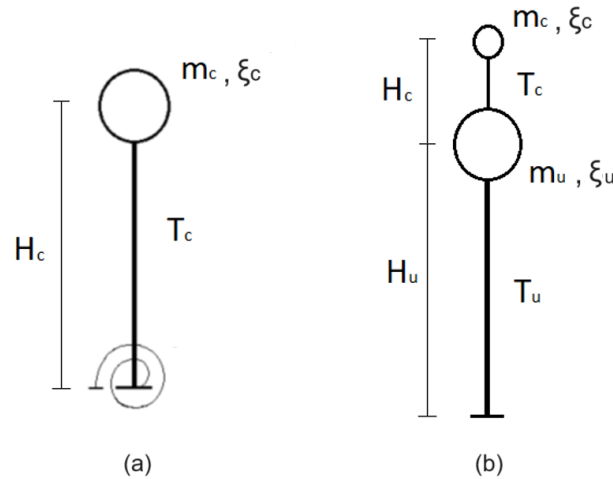


Figure 1. Equivalent models proposed: (a) One-Mass Model (OMM), for general usage, (b) Two-Mass Model (TMM), for nested component investigations.

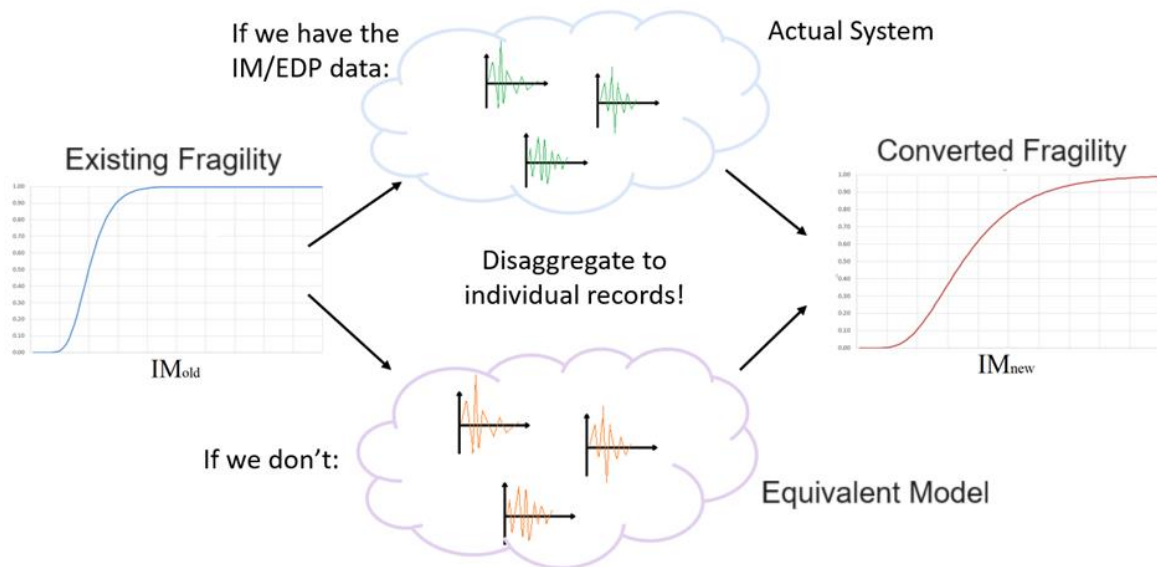


Figure 2. Visual representation of the IM conversion methodology. Ideally one has the IM-EDP values of the original full MDOF model to transform to any other IM of interest per the upper route. Lacking these, one should take the lower route and recreate consistent IM-EDP pairs via the equivalent model to be able to do the conversion.

3. IM Conversion examples

To evaluate the fidelity of the methodology presented, a nested component fragility conversion is examined. The component that will be studied is a service water pump found in the EPRI (2018) Technical Report. The most critical failure mode is referred to be the pump’s motor failure and thus the characteristics of the pump motor’s behaviour are used as the base properties for the component’s modelling. The equivalent model for

the component is a 3-D stick model and its characteristics are presented in Figure 3. The period is $T_c = 0.101\text{sec}$ with a damping of 5%. The mass is at 4.25Mg while the height of the component's model should be at 0.527m, to represent the motor. A nonlinear spring is applied at the base of the model with its properties reflecting the pushover results appearing also in Figure 3, while its ultimate displacement threshold is at $d_u = 2.9\text{mm}$. The above values were interpreted by the authors by examining the model's description in Annex U of EPRI (2018), so they should be representative of a realistic component case found in NPPs.

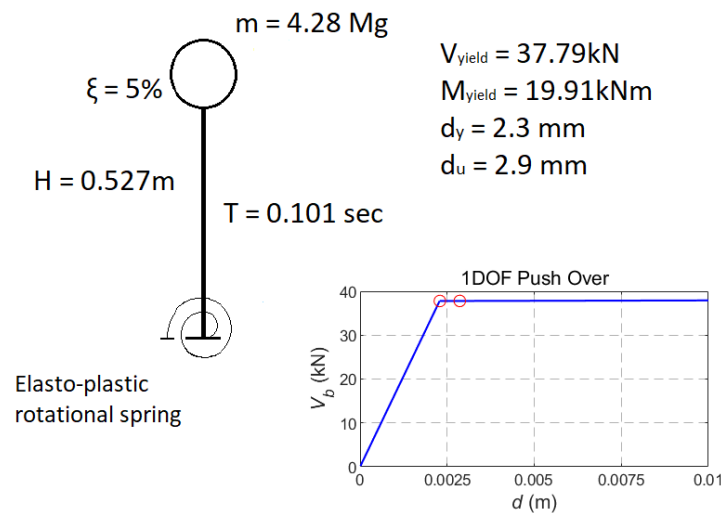


Figure 3. Service Water Pump characteristics, interpreted from Annex U of EPRI (2018).

The two case studies to be considered are (a) the component being nested in a high-strength high-stiffness industrial building, not too far from an NPP in terms of vibrational characteristics, and (b) the component being nested in a typical reactor structure found in EPRI (2007). Fragilities for both cases were calculated using the MDOF models of the structures. The actual MDOF fragilities were calculated for different IMs using the aforementioned d_u threshold and a record set of 30 ordinary (non-pulsive, non-long-duration) records. All IMs considered were estimated as the geometric mean of the two horizontal components. These are: (i) PGA as usually employed in NPP assessment, (ii) spectral acceleration at the period of the component $S_a(T_c)$, (iii) the geomean of multiple spectral acceleration values across a range of equally spaced periods, $AvgS_a$, with an increment selected here to be at 0.01s. Specifically, three period ranges were examined, namely $AvgS_a(0.05-0.15\text{sec})$, $AvgS_a(0.10-0.20\text{sec})$ and $AvgS_a(0.10-0.40\text{sec})$. Then, the equivalent model methodology was applied using both the OMM case, i.e., utilizing only the components properties (Figure 3) to build a one-mass stick model, and the TMM case (Figure 1b), whereby a model was built with the upper stick representing the component with its properties applied, while the lower stick has the properties of the understructure, namely its period, damping, and mass. Both understructures examined were linear, therefore an elastic element was used for the understructure as well. The equivalent models were then calibrated per their fragility in PGA terms to match the MDOF model's fragilities; then an IM conversion was applied to retrieve a representation of the component's fragilities in terms of all the aforementioned IMs, to validate the methodology.

3.1. Industrial Building

The first case study to be examined is the component being placed on the top floor of a one-story reinforced concrete (RC) building typical of industrial facilities, i.e., heavily overdesigned for fireproofing. The main characteristics of the building are its translational mode eigenperiods at 0.08sec in both X and Y directions, its storey height at 4.5m and its total mass at 173.75Mgr. A 5% damping was assigned in both its main translational modes. Due to its high strength the building remains elastic for all relevant seismic intensities. Using the building's MDOF model and by nesting the water pump component at its top floor, different fragilities were calculated for all the aforementioned IMs. An illustration of the building can be observed in Figure 4, while the interested reader may find more details for the model in Kazantzi *et al.* (2022).

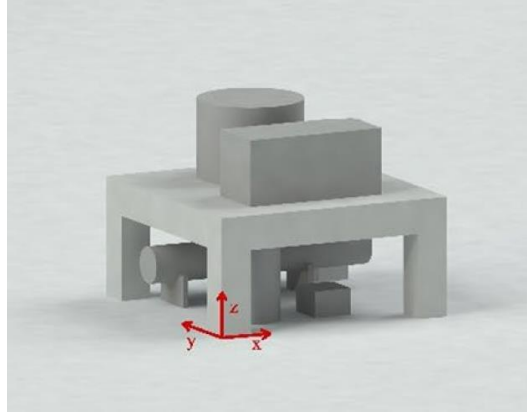


Figure 4. Schematic illustration of a one-storey RC industrial building (adopted from Kazantzi *et al.* 2022).

Exploiting the properties of the water pump and the building, the OMM and TMM were defined and calibrated according to the PGA fragility of the original MDOF model. The calibration parameters for each equivalent model are:

- For the OMM, $\alpha = 0.48$ and $\beta_\alpha = 0.25$; obviously disregarding the understructure required calibrations on both the fragility's median and dispersion for the equivalent model to match the MDOF results.
- For the TMM, $\alpha = 0.93$ and $\beta_\alpha = 0.01$, meaning that the equivalent model incorporating the understructure characteristics came very close to capturing the responses of the detailed MDOF model with relatively minor calibration in terms of the fragility's median value, while there was essentially no need to calibrate the dispersion.

Then, the IM conversion was performed using the equivalent models to calculate the fragilities based on the other IM types referenced. In Figures 5a–d the fragilities of the OMM and TMM equivalent models are illustrated, alongside the MDOF results, after matching the equivalent model's fragilities to the MDOF PGA fragility (Figure 5e). In Table 1 the lognormal fitting parameters for the fragilities are also presented. It is obvious that even though the OMM still calculated the medians correctly, there are deviations in the estimates of the dispersions. This is to be expected since the model uses only the properties of the component and disregards the effect of the eigenperiods of the understructure. On the other hand, the TMM captures all fragilities with a very good accuracy since the main characteristics of the building are included in the model, especially when considering that the building is not really affected by higher modes since it is a one storey structure. To make the improvement in the fragility calculations more apparent, the root-mean-square error (*RMSE*) between the original MDOF model fragilities and the equivalent model fragilities was calculated, as an indicator of how close the fragility curves are to each other:

$$RMSE = \sqrt{\frac{1}{n} \sum_{i=1}^n [F_{MDOF}(IM_i) - F_{ROM}(IM_i)]^2} \quad (1)$$

where $n = 150$ linearly-spaced values of IM_i are employed, ranging from 0 to 1.5g with an interval of 0.01g. $F_{MDOF}(\cdot)$ and $F_{ROM}(\cdot)$ are the fragilities of the original MDOF model and the reduced-order one.

The TMM effect on improving the results is obvious since, even the relatively small 3% deviation of the OMM fragility in terms of $S_a(T_c)$, becomes under 1% when using the TMM, indicating that this model is more suitable for nested-component fragilities. At the same time, it is shown that even under a heavy adjustment of the fragilities, as required by the OMM, one can expect reasonable accuracy in the end.

Table 1. Service water pump, nested in an industrial RC building: Median and dispersion of fragilities derived using equivalent models and compared to the original detailed model fragilities.

	MDOF		ONE-MASS MODEL			TWO-MASS MODEL		
	μ	σ	μ	σ	RMSE	μ	σ	RMSE
PGA	0.27	0.38	0.27	0.38	0.0%	0.27	0.39	0.6%
$S_a(T_c)$	0.45	0.20	0.45	0.27	2.9%	0.45	0.19	0.6%
Avg$S_a(0.05-0.15)$	0.44	0.23	0.43	0.29	2.2%	0.44	0.23	0.6%
Avg$S_a(0.10-0.20)$	0.53	0.28	0.53	0.31	1.6%	0.53	0.27	0.6%
Avg$S_a(0.10-0.40)$	0.54	0.37	0.53	0.39	0.6%	0.54	0.38	0.6%

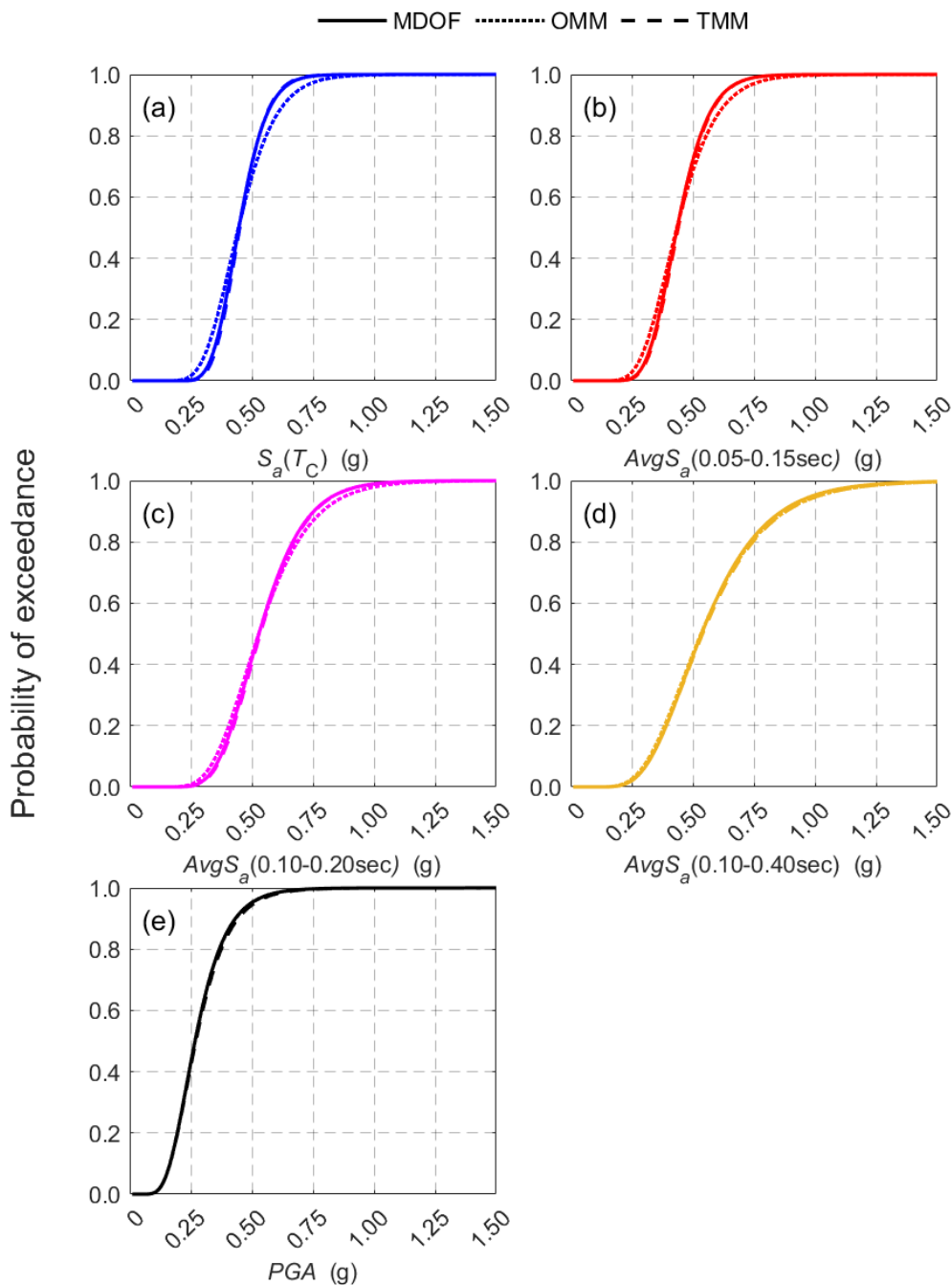


Figure 5. Service water pump, nested in an industrial RC building, fragility curves derived using equivalent models alongside the detailed model fragilities for (a) $S_a(T_c)$, (b) Avg $S_a(0.05 - 0.10sec)$, (c) Avg $S_a(0.10 - 0.20sec)$, (b) Avg $S_a(0.10 - 0.40sec)$ and (e) PGA.

3.2. Reactor structure

The second case study examined assumes that the service water pump component will be nested on top of the main containment/auxiliary building based on the AP 1000 advanced reactor design. The reduced order model used, consists of three concentric vertical sticks with basically no inter-connectivity at their higher elevations. The sticks represent the Coupled Auxiliary and Shield Building (ASB), the Steel Containment Vessel (SCV), and the Containment Internal Structure (CIS). The water pump component is assumed to be placed at the top node of the CIS vertical stick, therefore the properties of this part of the model were the ones incorporated for defining the understructure of the TMM. Specifically, the mass of the CIS “tower” was at 1330Mgr and its overall height at 33.10m, while the damping was defined at 7% according to the model’s description. Since the model is complex by its nature, to accurately acquire only the CIS “tower’s” eigenperiods, a free vibration test was employed, where a horizontal static load was applied to the top node of the “tower”, to then be instantaneously removed, to cause the tower to vibrate freely with its natural period. By using the Fourier transform in the resulting response displacement timehistory of the free vibration the main eigenperiods that characterize the CIS “tower” were defined at $T_x = 0.05\text{sec}$ and $T_y = 0.04\text{sec}$. For more information for the model the interested reader can refer to Gerontati and Vamvatsikos (2023) and originally to EPRI (2007). It should be noted though that for calculating the MDOF fragilities for all the aforementioned IM types, the full reactor model was employed by of course modeling the nested pump at the top of the CIS “tower”.

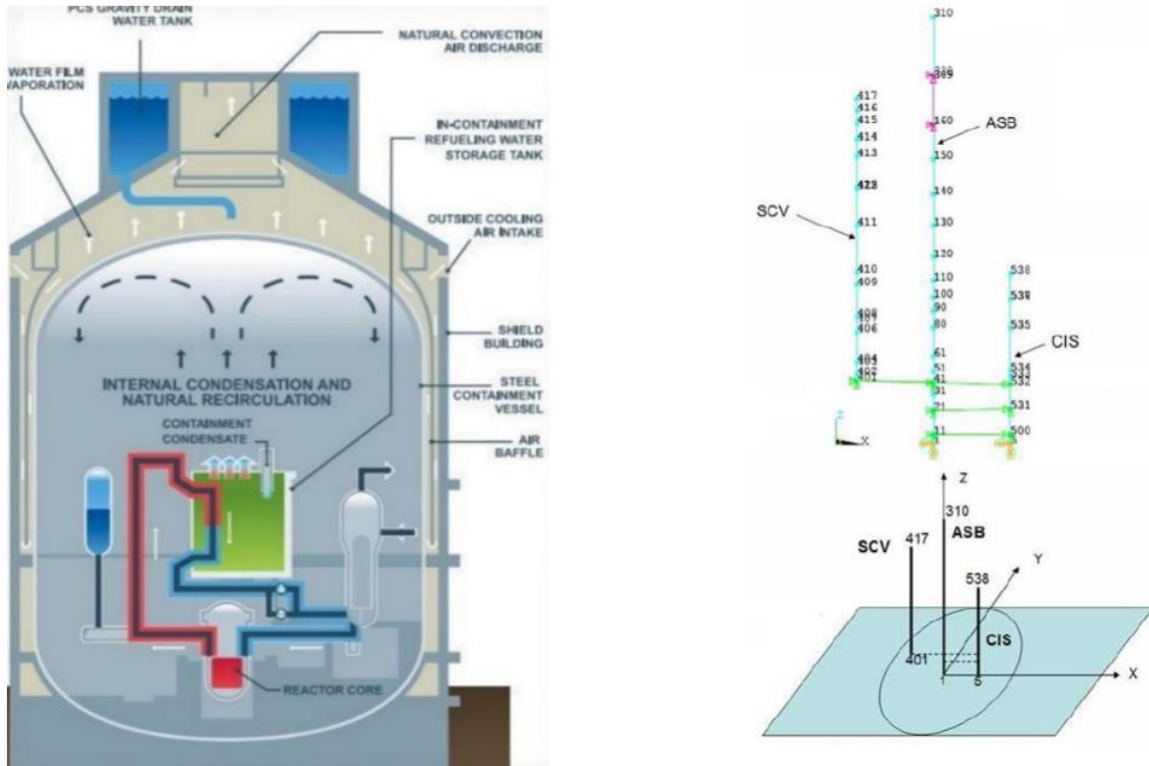


Figure 6. Schematic illustration of the original AP1000 reactor design (left) and the reduced order stick model (right) per EPRI (2007).

Using again the properties of the service water pump and the CIS “tower”, the OMM and TMM were defined and calibrated according to the PGA fragility of the original MDOF model. The calibration parameters for each the models are:

- For the OMM, $\alpha = 0.88$ and $\beta_\alpha = 0.10$; disregarding the understructure required some moderate calibration of both the fragility’s median and dispersion for the equivalent model to match the MDOF.
- For the TMM, $\alpha = 1.04$ and $\beta_\alpha = 0.10$, the equivalent model requires a lower multiplier (i.e., closer to 1.0) for the adjustment of the fragility’s median but required the same additional dispersion to match the MDOF’s PGA fragility.

Table 2. Service water pump, nested in the reactor structure: Median and dispersion of fragilities of the derived using equivalent one/two-mass models versus the detailed model results.

	MDOF		ONE-MASS MODEL			TWO-MASS MODEL		
	μ	σ	μ	σ	RMSE	μ	σ	RMSE
PGA	0.47	0.31	0.47	0.28	1.3%	0.47	0.29	1.0%
$S_a(T_C)$	0.74	0.13	0.79	0.14	6.8%	0.77	0.12	4.6%
Avg $S_a(0.05-0.15)$	0.73	0.18	0.77	0.16	5.1%	0.76	0.16	3.2%
Avg $S_a(0.10-0.20)$	0.85	0.19	0.94	0.20	9.1%	0.92	0.21	7.2%
Avg $S_a(0.10-0.40)$	0.89	0.30	0.95	0.30	4.7%	0.93	0.31	3.2%

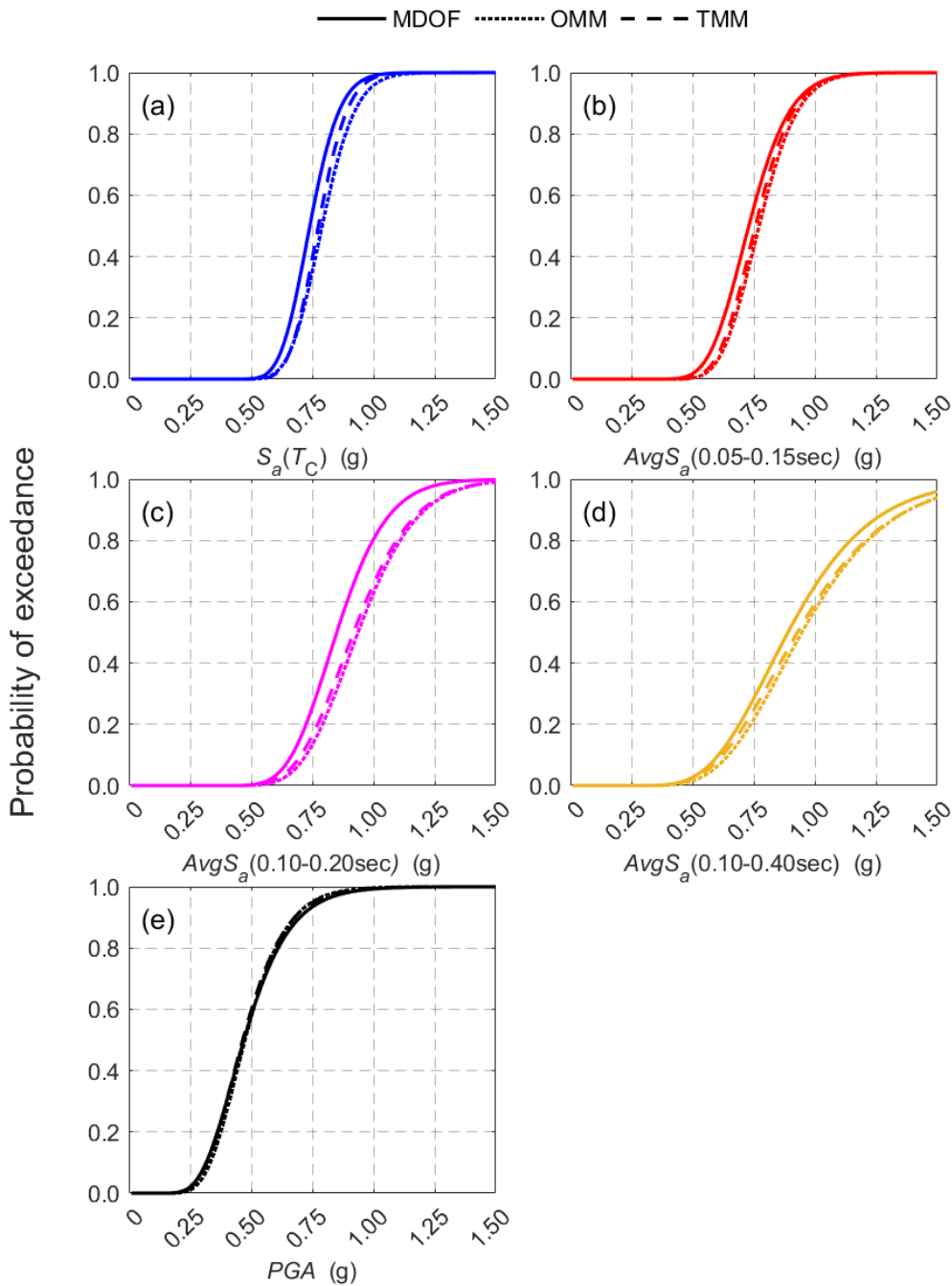


Figure 7. Service water pump, nested in a reactor structure, fragilities derived using equivalent models for (a) $S_a(T_C)$, (b) Avg $S_a(0.05 - 0.10$ sec), (c) Avg $S_a(0.10 - 0.20$ sec), (b) Avg $S_a(0.10 - 0.40$ sec) and (e) PGA.

In Figures 7a–d the fragilities of the OMM and TMM equivalent models are illustrated, after performing an IM conversion to the calibrated equivalent model fragilities, using the MDOF PGA fragility (Figure 7e) as a basis. In Table 2 the lognormal fitting parameters for the fragilities are also presented. In this case due to the complexity of the structure both the OMM and TMM produce fragilities that slightly deviate from what the original model fragilities would be. This is normally due to the reactor being characterized by many different translational and non-translational complex eigenmodes, some of which do and some of which do not contribute to the component's response. In any case, though, the RSME values calculated indicate relatively small deviations regardless, with the worst cases remaining under 10%. Moreover, the equivalent models incorporated both calculate the fragility dispersions quite accurately, with the deviations from the detailed MDOF fragilities being mainly attributed in this case to the median estimates of the equivalent models. This means that even for more complex models, the methodology could still provide a good estimate of the fragilities that would be acquired through a detailed process of IM conversion for the original fragilities. It should also be noted, that even in this case, the RMSE indicators point at the TMM approach as the more “accurate” one, compared with the more simplistic (but maybe still usable in some cases) OMM model, at least when applying this methodology for component fragilities.

4. Conclusions

The re-evaluation of the nuclear power plant facilities seismic assessment methodologies should be an always relevant discussion, as the engineering community strives to safeguard some of the highest-importance infrastructure. Naturally, the incorporation of the advancements in IM selection for a more reliable assessment should not be disregarded. To clarify the roadmap for any future advancements, simplified methodologies can be incorporated as a first stage investigation of the direction of such shifts in perspective. The exploitation of equivalent models anchored to the existing fragilities to reproduce seismic responses that allow for intensity measure conversions, can be a good first step into exploring different intensity measure types for the assessment of the structures and components found in a nuclear power plant. In both case studies evaluated herein, i.e. a service water pump component nested in an industrial reinforced concrete building or a reactor structure, the component fragilities were reproduced successfully in PGA terms with the conversion into other IM types yielding satisfactory results as well. Of the two equivalent models tested, the one-mass and the two-mass model, it seems that for an investigation related to non-structural components, the two-mass model, incorporating both the component's and the understructure's properties, is the better choice, improving the fidelity of the estimated fragility results relative to the original MDOF model fragilities.

5. Acknowledgements

Financial support has been provided by the European Commission through the Program "METIS – Methods and tools innovations for seismic risk assessment" with Grant Agreement number 945121 and by the European Framework Programme for Research and Innovation under the “YADES” Marie Skłodowska-Curie project with Grant Agreement No 872931.

6. References

- Adam C., Kampenhuber D., Ibarra L.F., Tsantaki S. (2017). Optimal spectral acceleration-based intensity measure for seismic collapse assessment of P-delta vulnerable frame structures. *Journal of Earthquake Engineering*, 21(7): 1189-1195.
- Bakalis K., Kohrangi M., Vamvatsikos D. (2018). Seismic intensity measures for above-ground liquid storage tanks. *Earthquake Engineering & Structural Dynamics*, 47(9): 1844-1863.
- Bakalis K., Vamvatsikos D. (2018). Seismic fragility functions via nonlinear response history analysis. *Journal of Structural Engineering (ASCE)*, 144 (10): 04018181. [https://doi.org/10.1061/\(ASCE\)ST.1943-541X.0002141](https://doi.org/10.1061/(ASCE)ST.1943-541X.0002141)
- Bojórquez E., Iervolino I. (2011). Spectral shape proxies and nonlinear structural response. *Soil Dynamics and Earthquake Engineering*, 31(7): 996-1008.
- Crowley H., Dabbeek J., Despotaki V., Rodrigues D., Martins L., Silva V., Romão X., Pereira N., Weatherill G., Danciu L. (2021). European Seismic Risk Model (ESRM20). *EFEHR Technical Report 002 V1.0.0*. <https://doi.org/10.7414/EUC-EFEHR-TR002-ESRM20>

- Eads L., Miranda E., Lignos D.G. (2015). Average spectral acceleration as an intensity measure for collapse risk assessment. *Earthquake Engineering & Structural Dynamics*, 44(12): 2057-2073.
- EPRI (2007). Program on Technology Innovation: *Validation of CLASSI and SASSI Codes to Treat Seismic Wave Incoherence in Soil-Structure Interaction (SSI) Analysis of Nuclear Power Plant Structures*. EPRI, Palo Alto, CA: 2007. 1015111.
- EPRI (2018). Program on Technology Innovation: *Seismic Fragility and Seismic Margin Guidance for Seismic Probabilistic Risk Assessments*. EPRI, Palo Alto, CA: 2018. 3002012994.
- Gerontati A.V., Vamvatsikos D. (2023). The effect of intensity measure selection and epistemic uncertainties on the estimated seismic performance for non-structural components of nuclear power plants. *Proceedings of the SECED 2023 Conference*, Cambridge, UK, 2023.
- Heresi P., Miranda E. (2021). Intensity measures for regional seismic risk assessment of low-rise wood-frame residential construction. *Journal of Structural Engineering*, 147(1): 04020287.
- Karaferis N.D., Vamvatsikos D. (2022). Intensity measure transformation of fragility curves for 2D buildings using simplified models. *Proceedings of the 3rd European Conference on Earthquake Engineering & Seismology*, Bucharest, Romania, 2022.
- Karaferis N.D., Vamvatsikos D. (2023). Fragility curve disaggregation examples for localized measures of response. *Proceedings of the SECED 2023 Conference*, Cambridge, UK, 2023.
- Kazantzi A.K., Karaferis N.D., Melissianos V.E., Bakalis K., Vamvatsikos D. (2022). Seismic fragility assessment of building-type structures in oil refineries. *Bulletin of Earthquake Engineering*, 20(12), 6853-6876. <https://doi.org/10.1007/s10518-022-01476-y>
- Kazantzi A.K., Vamvatsikos D. (2015). Intensity measure selection for vulnerability studies of building classes. *Earthquake Engineering and Structural Dynamics*, 44(15): 2677-2694.
- Kohrangi M., Bazzurro P., Vamvatsikos D. (2016). Vector and scalar IMs in structural response estimation, part II: building demand assessment. *Earthquake Spectra*, 32(3): 1525-1543.
- Lachanas C.G., Vamvatsikos D., Dimitrakopoulos E.G. (2023). Intensity measures as interfacing variables versus response proxies: The case of rigid rocking blocks. *Earthquake Engineering & Structural Dynamics*, 52(6): 1722-1739.
- Luco N., Cornell C.A. (2007). Structure-specific scalar intensity measures for near-source and ordinary earthquake ground motions. *Earthquake Spectra*, 23(2): 357-392.
- O'Reilly G.J. (2021). Seismic intensity measures for risk assessment of bridges. *Bulletin of Earthquake Engineering*, 19(9): 3671-3699.
- Rosti A., Del Gaudio C., Rota M., Ricci P., Di Ludovico M., Penna A., Verderame G.M. (2021). Empirical fragility curves for Italian residential RC buildings. *Bulletin of Earthquake Engineering*, 19(8), 3165-3183. <https://doi.org/10.1007/s10518-020-00971-4>
- Silva V., Akkar S., Baker J.W., Bazzurro P., Castro J.M., Crowley H., Dolsek M., Galasso C., Lagomarsino, R., Monteiro S., Perrone D., Pitilakis K., Vamvatsikos D. (2019). Current challenges and future trends in analytical fragility and vulnerability modelling. *Earthquake Spectra*, 35 (4): 1927-1952. <https://doi.org/10.1193/042418EQS1010>
- Stefanidou S.P., Kappos A.J. (2017). Methodology for the development of bridge-specific fragility curves, *Earthquake Engineering & Structural Dynamics*, 46(1), 73-93. <https://doi.org/10.1002/eqe.2774>
- Vamvatsikos D., Cornell C.A. (2002). Incremental dynamic analysis. *Earthquake Engineering and Structural Dynamics*, 31(3): 491-514. <https://doi.org/10.1002/eqe.141>
- Vamvatsikos D., Cornell C.A. (2005). Developing efficient scalar and vector intensity measures for IDA capacity estimation by incorporating elastic spectral shape information. *Earthquake Engineering and Structural Dynamics*, 34: 1573-1600. <https://doi.org/10.1002/eqe.496>
- Zentner I., Humbert N., Ravet S., Viallet E. (2011). Numerical methods for seismic fragility analysis of structures and components in nuclear industry - Application to a reactor coolant system. *Georisk*, 5(2): 99-109. <https://doi.org/10.1080/17499511003630512>